Accepted Manuscript

Monoacylglycerol lipase blockade impairs fine motor coordination and triggers cerebellar neuroinflammation through cyclooxygenase-2

Sara Martínez-Torres, Laura Cutando, Antoni Pastor, Ako Kato, Kenji Sakimura, Rafael de la Torre, Emmanuel Valjent, Rafael Maldonado, Masanobu Kano, Andrés Ozaita
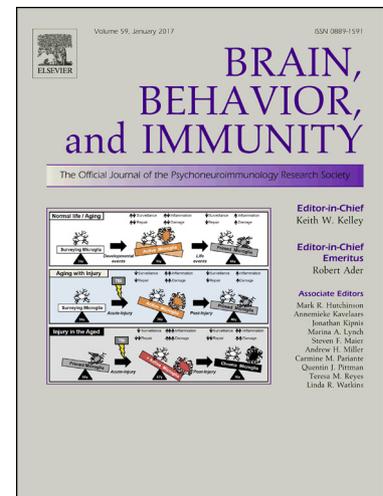
Monoacylglycerol lipase blockade impairs fine motor coordination and triggers cerebellar neuroinflammation through cyclooxygenase-2

Abbreviated title: Differential effect of MAGL blockade on neuroinflammation

Sara Martínez-Torres[1]*, Laura Cutando[1,5]*, Antoni Pastor[2], Ako Kato[4], Kenji Sakimura[3], Rafael de la Torre[2], Emmanuel Valjent[5], Rafael Maldonado[1], Masanobu Kano[4], Andrés Ozaita[1]#

[1] Laboratory of Neuropharmacology-NeuroPhar, Department of Experimental and Health Sciences. University Pompeu Fabra, Barcelona, Spain.
[2] Integrative Pharmacology and Systems Neuroscience, IMIM-Hospital del Mar Medical Research Institute, Barcelona, Spain
[3] Department of Cellular Neurobiology, Brain Research Institute, Niigata University, Niigata 951-8585, Japan
[4] Department of Neurophysiology, Graduate School of Medicine, The University of Tokyo, Tokyo 113-0033, Japan
[5] IGF, CNRS, INSERM, University of Montpellier, Montpellier, France.

*equal contribution

#Corresponding author: Andrés Ozaita, Laboratori de Neurofarmacologia, Facultat de Ciències de la Salut i de la Vida, Universitat Pompeu Fabra, Parc de Recerca Biomèdica de Barcelona, C/ Doctor Aiguader 88, 08003 Barcelona, Spain. Phone: +34-93-3160823; Fax: + 34-93-3160901; e-mail: andres.ozaita@upf.edu

Keywords: Monoacylglycerol lipase, 2-arachidonoylglycerol, microglia, cyclooxygenase-2, cerebellum, motor coordination, neuroinflammation, prostaglandins, hippocampus.

Word count: 8517

1

Highlights

1. Monoacylglycerol lipase (MAGL) inactivation increases microglial perimeter in the cerebellum.

2. Cerebellar microglia activation concurs with COX-2 over-expression and motor deficits.

3. COX-2 inhibition prevents the cerebellar neuroinflammation caused by MAGL deletion.

4. MAGL depletion decreased AA and PGs levels in the cerebellum and hippocampus.

5. Regional differences in MAGL inhibition outcome caution endocannabinoid targeting.

Abstract

Monoacylglycerol lipase (MAGL) is the main enzyme implicated in the degradation of the most abundant endocannabinoid in the brain, 2-arachidonoylglycerol (2-AG), producing arachidonic acid (AA) and glycerol. MAGL pharmacological inhibition with JZL184 or genetic deletion results in an exacerbated 2-AG signaling and reduced synthesis of prostaglandins (PGs), due to the reduced AA precursor levels. We found that acute JZL184 administration, previously described to exert anti-inflammatory effects, and MAGL knockout (KO) mice display cerebellar, but not hippocampal, microglial reactivity, accompanied with increased expression of the mRNA levels of neuroinflammatory markers, such as cyclooxygenase-2 (COX-2). Notably, this neuroinflammatory phenotype correlated with relevant motor coordination impairment in the beam-walking and the footprint tests. Treatment with the COX-2 inhibitor NS398 during 5 days prevented the deficits in cerebellar function and the cerebellar microglia reactivity in MAGL KO, without affecting hippocampal reactivity. Altogether, this study reveals the brain region-specific response to MAGL inhibition, with an important role of COX-2 in the cerebellar deficits associated, which should be taken into account for the use of MAGL inhibitors as anti-inflammatory drugs.

1. Introduction

The endocannabinoid system (ECS) is an important neuromodulatory system involved in multiple physiological brain functions, including motor coordination (Kano et al., 2009). Exogenous or endogenous ligands (endocannabinoids) modulate this system by binding to cannabinoid receptors highly expressed in the central nervous system (CNS). The endocannabinoids, 2-arachidonoylglycerol (2-AG) and arachidonoylethanolamine (AEA or anandamide), are produced in an activity-dependent manner by specific synthesis enzymes, while their signaling is reduced by the activity of hydrolysis enzymes (Blankman et al., 2007; Cravatt et al., 1996). 2-AG is known to function as a retrograde messenger at synapses and mediate both short-term and long-term depression of excitatory and inhibitory synaptic transmission throughout the CNS (Gao et al., 2010; Ohno-Shosaku and Kano, 2014; Tanimura et al., 2010). The main enzyme implicated in 2-AG hydrolysis *in vivo* is monoacylglycerol lipase (MAGL) (Dinh et al., 2002; Savinainen et al., 2012). MAGL is localized in the cytoplasm of subsets of presynaptic terminals in different brain areas including the cerebellum (Tanimura et al., 2012) and hippocampus (Uchigashima et al., 2011). It accounts for 85% of 2-AG metabolism producing arachidonic acid (AA) and glycerol as products (Dinh et al., 2002; Savinainen et al., 2012). The remaining 15% of 2-AG is mainly metabolized by α/β-hydrolase domain-containing 6 (ABHD6) and, to a minor extent, by cyclooxygenase-2 (COX-2) (Blankman et al., 2007). COX-2 is an inducible enzyme involved in inflammatory responses (Vane and Botting, 1998) converting AA into prostaglandins (Urquhart et al., 2015). In addition, COX-2 may produce highly unstable prostaglandin-glycerol esters (PG-G) from 2-AG, with a relevant role in inflammatory response (Morgan et al., 2018).

Pharmacological and genetic inactivation of MAGL was shown to exert anti-inflammatory actions in the brain by reducing the synthesis of pro-inflammatory mediators, specifically the eicosanoids derived from AA (Nomura et al., 2011). Under such conditions, hippocampal microglia that would respond to lipopolysaccharide injection did not show signs of activation (Nomura et al., 2011). Accordingly, MAGL inhibition using JZL184 administration after a mild traumatic brain injury protected blood-brain barrier integrity and improved neurological and behavioral functions (Katz et al., 2015). Similarly, MAGL inactivation by JZL184 decreased microglial reactivity in the hippocampus in a mouse model of Alzheimer's disease (Pihlaja et al., 2015). These promising features of JZL184 contrast with previous results from our group demonstrating the presence of activated microglia and pro-inflammatory mediators with the increase of the cannabinergic tone after repeated exposure to the exogenous cannabinoid agonist delta9-tetrahydrocannabinol. These inflammatory alterations were localized specifically in the cerebellum, but not in other brain regions, and were associated with deficits in fine motor coordination and cerebellar learning-tasks (Cutando et al., 2013).

In this study, we report that MAGL pharmacological or genetic inhibition results in significant deficits in motor coordination, enhanced microglial reactivity selectively in the cerebellar molecular layer, and increased expression of cerebellar COX-2 and pro-inflammatory mediators. These cerebellar alterations, which are not observed in the hippocampus, are partially prevented with the administration of the selective COX-2 inhibitor NS398 in MAGL KO mice. Altogether these data suggest the profound role of the ECS in the control of brain homeostasis at different brain regions and the particular sensitivity of the cerebellum in the regulation of the neuronal-glia circuitry.

5

2. Materials and Methods

2.1. Animals

All experiments were performed in male mice between 8 and 16 weeks of age. MAGL knockout mice (MAGL KO) and wild-type (WT) littermates in C57BL/6J genetic background were obtained and genotyped as previously described (Uchigashima et al., 2011). For JZL184 treatment we used C57BL/6J male mice (Charles River). Mice were housed in cages of four and maintained at controlled temperature (21 ± 1ºC) and humidity (55 ± 10%) environment. Food and water were available *ad libitum*. Lighting was maintained at 12-hour cycles (on at 8:00 am and off at 8:00 pm.).

All animal procedures were conducted following ARRIVE (Animals in Research: Reporting Experiments) guidelines (Kilkenny et al., 2010) and standing guidelines (European Communities Directive 2010/63/EU). Procedures were approved by the local ethical committee (Comitè Ètic d'Experimentació Animal-Parc de Recerca Biomèdica de Barcelona, CEEA-PRBB). All behavioral experiments were conducted under experimental conditions blind to the observer.

2.2. Drugs and treatments

JZL184 (Abcam) and NS398 (Tocris Bioscience) were diluted in 15% dimethyl sulfoxide (DMSO; Scharlau Chemie), 4.25% polyethylene glycol 400 (Sigma-Aldrich), 4.25% Tween-80 (Sigma-Aldrich) and 76.5% saline. JZL184 and NS398 were administered intraperitoneally (i.p.) in a volume of 5 mL/kg and 10 mL/kg of body weight respectively. JZL184 was injected 6 h before behavioral and biochemical analysis. NS398 was injected during 5 days and 2 h prior to

experimental procedures. Mice were randomly assigned to experimental groups.

2.3. Motor coordination tests

2.3.1. Beam walking test

Mice were trained to cross a horizontal wooden circle rod (1 m long, 3 cm in diameter) placed 60 cm above a cushioned table during 2 days before the test (3 times per day). The day of the test, mice crossed a wide wooden rod (3 cm in diameter) and a narrow wooden rod (1 cm in diameter). The latency to cross the rods and the total number of foot-slips were recorded and used to calculate the mean latency time and the mean number of foot-slips for each experimental group.

2.3.2. Footprint test

Mouse's paws were coated with non-toxic color inks. Mice were allowed to walk down an open-top narrow runway covered with white paper. The runway was 50 cm long and 10 cm wide, flanked with 10 cm side walls. Mice were trained twice per day during the 2 days previous to the day of the test. To ease the measurements, front and hind paws were coated with different colors. A total of 2 trials were performed on each mouse. Once the footprints had dried, the following parameters were measured: base width (front base and hind base), overlap width (left overlap, right overlap), left and right forelimb stride and left and right hindlimb stride (8 steps for each mouse were analyzed). The means for each parameter were calculated for each experimental group.

7

2.4. Immunofluorescence studies

Mice were deeply anesthetized with a mixture of ketamine (100mg/kg)/xylazine (20mg/kg) by i.p. injection (0.2mL/10g of body weight), before to intracardiac perfusion of 4% (wt/vol) paraformaldehyde/0.1M phosphate buffer pH 7.4 (PB) for immunofluorescence microscopy. Brains were removed and post-fixed overnight at 4°C in the same fixative solution. Brain sections (30 µm) were cut with a vibratome (VT1000S; Leica) and kept in a solution containing 30% ethylene glycol (Sigma-Aldrich), 30% glycerol (Merck-Millipore), and PB at – 20°C until processed for immunofluorescence analysis.

Free-floating slices were rinsed in PB, incubated for 15 min in 0.2 % Triton X-100 in PB, and then incubated overnight at 4°C with primary antibody anti-Iba1 (1:500; Wako). The next day, after 2 rinses of 10 min in PB, sections were incubated for 2 h at room temperature with the fluorescent anti-rabbit-Cy3 (1:500; Jackson ImmunoResearch Laboratories). After 3 washes of 10 min, tissue sections were mounted onto gelatin-coated glass slides with Mowiol mounting media (0.5 M Mowiol 40-88 (Sigma-Aldrich), 20 % glycerol (Merck-Millipore), 0.1 M Tris pH 8.5).

2.5. Image analysis

To evaluate the changes in microglial morphology, confocal microscopy images of whole microglial cells stained with Iba1 were acquired with an oil immersion lens (×40 objective; 1.5 zoom). Images were taken at different z levels (0.3 µm depth intervals) to evaluate the morphology of the whole cell. Afterwards, the perimeter of the microglial soma was analyzed with ImageJ software (NIH). We evaluated 10 cells per animal and 3-6 animals per genotype (30-60 cells per genotype).

2.6.Analysis of endocannabinoids, prostaglandins, and arachidonic acid from brain tissue.

The analysis of endocannabinoids was done as previously described by LC/MS-MS (Navarro-Romero et al., 2019). We analyzed prostaglandin-E2 (PGE$_2$), prostaglandin-D2 (PGD$_2$), and AA by LC/MS-MS using similar methodology than endocannabinoids analysis. Half-left hippocampus (15.9 ± 1.0 mg) and half-left cerebellum (29.1 ± 3.3 mg) of mice were placed in a 1 mL Wheaton glass homogenizer and spiked with 25 µL of a mix of deuterated internal standards dissolved in acetonitrile. The mix contained 0.1 µg/mL PGD2-d4 (Cayman Chemical) and 25 µg/mL AA-8 (Cayman Chemical). Tissues were homogenized on ice with 700 µL a mixture of 50 mM Tris-HCl buffer (pH 7.4): methanol (1:1) and the homogenates were transferred to 12 mL glass tubes. The homogenizer was washed twice with 0.9 mL of the same mixture and the contents were combined into the tube giving an approximate volume of 2.5 mL of homogenate. The homogenization process took less than 5 min per sample and homogenates were kept on ice until organic extraction to minimize PGs degradation. Next, homogenates were extracted with 5 mL chloroform and tubes were centrifuged. The lower organic phase was transferred to clean glass tubes, evaporated under a stream of nitrogen in a 39ºC water bath and extracts were reconstituted in 100 µL of a mixture water: acetonitrile (50:50, v/v) with 0.01% formic acid (v/v) and transferred to high performance liquid chromatography vials with glass microvials. Ten µL of extract were injected into the LC/MS-MS system. PGs were separated using a Waters Acquity UPLC® system with a Xevo TQ-Smicro MS detector. Chromatographic separation was carried out with a Waters ACQUITY UPLC® CSH™ Phenyl-Hexyl column (2.1 x 100 mm, 1.7 µm particle size) maintained at 55ºC with a mobile phase flow rate

9

of 0.4 mL/min. The composition of the mobile phase was: A: 0.01% (v/v) formic acid in water; B: 0.01% (v/v) formic acid in acetonitrile. PGD_2, PGE_2 and AA were separated by gradient chromatography (Supplementary Figure 1). The initial conditions were 20% B for 1 min. The gradient was first increased linearly to 65% B over 10 min, then increased linearly to 100% B over 3 min and maintained at 100% B for 2.5 min, to return to initial conditions for a further 1.5 min with a total run time of 18 min. The ion source was operated in the negative electrospray mode. The source voltages were 3 KV for the capillary and 25V for the cone. Source desolvation temperature was set at 600ºC. The source gas flow was set at 1200 L/h for desolvation and 50 L/h for the cone. The following precursor to product m/z ions were used for quantification each with the following different collision energies (CE): AA m/z 303>259 CE, 10V, AA-d8 m/z 311>267 CE 10V, PGD2/PGE2 m/z 351>271 CE 15V, PGD2-d4 m/z 355 >275 CE 15V. Quantification was done by isotope dilution with the response of the internal standards.

2.7. RNA isolation and qRT-PCR analysis

Hippocampal and cerebellar tissues were dissected and stored at -80°C. Isolation of total RNA was performed using an RNeasy Mini kit (QIAGEN) according to the manufacturer's instructions. The quality and concentration of the total RNA was assessed using Nanodrop 1000 spectrophotometer. Reverse transcription was performed with 0.25 µg of total RNA from each animal to produce cDNA in a 20 µL reaction with 4 µl of SuperScript® VILO™ cDNA synthesis kit (Thermo Fisher Scientific). Resulting cDNA was used to perform quantitative real-time PCR (qRT-PCR) analysis on the LC480 Real-Time PCR System (Roche), together with SYBR Green PCR master mix and the primer

10

sequences listed below. Analysis was performed using LightCycler® 480 Software (Roche). Data are expressed as the fold change comparing WT and MAGL KO samples. All the samples were tested in triplicate, and the relative expression values were normalized to the expression value of *Tbp2α* (for the cerebellar samples) and *Actb* (for the hippocampal samples). The primer sequences used for *Abhd6*, *Cox2*, *Cnr1, Cnr2, Ilb1*, *Itgam*, *Tnfa, Actb* and *Tbp2α* are indicated in the Supplementary Table 1.

2.8. Statistical analysis

The statistical significance was assessed using unpaired Student's *t*-test, one-way ANOVA or two-way ANOVA followed by a posteriori Bonferroni *post-hoc* when appropriate. The Pearson correlation coefficient was used to analyze the relationship between motor coordination alterations and the perimeter of microglial soma. All data were analyzed using GraphPad Prism Software. Data are presented as the mean ± SEM. P values of less than 0.05 were considered significant. Outliers (±2 SD from the mean) were excluded.

3. Results

3.1. Acute JZL184 treatment results in motor coordination deficits

We analyzed the effects of acute MAGL inhibition on motor coordination under the same treatment conditions (40 mg/kg, i.p.) used to reveal anti-inflammatory effects of JZL184 in total brain homogenates and hippocampal sections (Nomura et al., 2011). In parallel, we also assessed a dose of JZL184 5 times lower (8 mg/kg) previously characterized in our group to significantly modify the brain content of 2-AG (Busquets-Garcia et al., 2011; Saravia et al., 2017).

We used the beam walking test and the footprint test to evaluate the motor coordination in mice treated with JZL184 (8 or 40 mg/kg) using vehicle-injected mice as controls. The beam walking test revealed a significant dose-related motor impairment both in the wide beam ($F_{(2,14)} = 8.244$, $p < 0.01$) and the narrow beam ($F_{(2,16)} = 5.262$, $p < 0.05$) (Figure 1A). We found that mice treated with the lowest dose of JZL184 (8 mg/kg) showed an increased number of foot-slips in comparison to the vehicle-treated group when they crossed the wide beam ($p < 0.05$) (Figure 1A). This significant difference was exacerbated when mice were treated with the highest dose of JZL184 (40 mg/kg) ($p < 0.01$). When the narrow beam was tested, both JZL184 treated-groups performed a higher number of foot-slips in comparison to the control group ($F_{(2,16)} = 5.262$, $p < 0.05$) (Figure 1A). In the footprint test, JZL184 produced motor coordination impairment only when was administered at the dose of 40 mg/kg. JZL184 (40 mg/kg). Treated-mice presented significant shorter stride length than vehicle-treated mice (L forelimb: $F_{(2,18)} = 3.112$, $p = 0.069$; NS; R forelimb: $F_{(2, 18)} = 3.991$, $p < 0.05$; L hindlimb: $F_{(2,18)} = 4.201$, $p < 0.05$; R hindlimb: $F_{(2,18)} = 4.120$, $p < 0.05$) (Figure 1B). However, no significant differences were found in

the base width (front base and hind base) neither in the overlap width (left overlap and right overlap) (data not shown).

3.2. Acute JZL184 treatment results in cerebellar inflammation

We next evaluated whether JZL184 administration would affect microglial morphology. Thus, an increase of the soma perimeter was found in cerebellar Iba1-positive cells of JZL184 treated-groups ($F_{(2, 17)} = 4.99$, $p < 0.05$), reaching a significant post-hoc difference at the dose of 40 mg/kg ($p < 0.05$) (Figure 2A). Notably, the microglial activation was not detectable in other brain regions, such as the CA3 region of the dorsal hippocampus (Figure 2B), where MAGL is heavily expressed (Rivera et al., 2014). Next, we assessed whether the bushy microglial morphology observed in the JZL184 treated-mice was accompanied by changes in the expression of the microglial activation marker CD11b (*Itgam*) and the pro-inflammatory markers interleukin-1B (*Ilb1*) and tumor necrosis factor α (*Tnfa*). Quantitative real time PCR (qRT-PCR) analysis showed a significant treatment effect ($F_{(2, 13)} = 4.228$, $p < 0.05$) to increase the *Itgam* mRNA expression in the cerebellum of JZL184 treated-mice evaluated by one-way ANOVA test. However, Bonferroni *post-hoc* analysis did not reveal significant changes in *Itgam* mRNA expression between mice treated with vehicle and those treated with JZL184 at the dose of 8 mg/kg ($p = 0.09$; NS) and 40 mg/kg ($p = 0.07$; NS) (Figure 2C). This pro-inflammatory marker was not increased in the hippocampus of JZL184 treated-mice (Figure 2D).

Similarly, the expression of *Ilb1* and *Tnfa* showed a non-significant trend to increase in the cerebellum of the JZL184 treated-groups (*Ilb1*: $F_{(2, 12)} = 3.035$, $p = 0.086$; NS; *Tnfa*: $F_{(2, 12)} = 2.419$, $p = 0.131$; NS) (Supplementary Figure 2A), without modifications in the hippocampus (Supplementary Figure 2B). The

expression of *Cnr1* did not change after JZL184 treatment in the hippocampus and cerebellum (Supplementary Figure 2, C and D). MAGL is the main enzyme involved in the degradation of 2-AG, but other lipases such as ABHD6 are involved in the metabolism of this endocannabinoid. In addition, considering that neuronal COX-2 can produce PG-Gs in the brain when 2-AG levels are enhanced (Morgan et al., 2018), we analyzed the mRNA expression levels of *Cox2* and *Abhd6* after the acute JZL184 treatment. Quantitative analysis of *Cox2* showed a significant treatment effect in the cerebellum of JZL184 treated-mice ($F_{(2,13)}$ = 3.98, $p < 0.05$) with a significant *post-hoc* increase between vehicle and JZL184 40 mg/kg group ($p < 0.05$). Significant changes of *Abhd6* mRNA expression in the cerebellum between vehicle and JZL184 treated-group were also observed ($F_{(2,13)}$ = 7.616 $p < 0.01$) (Figure 2E). Interestingly, only *Abhd6* ($F_{(2,14)}$ = 8.601 $p < 0.01$), but not *Cox2*, was elevated in the hippocampus of JZL184 treated-mice (Figure 2F). Together, these results reveal a differential sensitivity of the cerebellum to the inflammatory process promoted by the deregulation of 2-AG levels.

3.3. MAGL deletion produces motor coordination impairment and cerebellar inflammation

To evaluate the relevance of MAGL deletion in the behavioral and inflammatory alterations that are revealed with JZL184, we investigated the motor coordination performance and the microglial reactivity in MAGL KO and in WT littermates. MAGL KO mice performed a significantly higher number of foot-slips when they crossed the wide beam ($t_{(18)}$ = 4.699, $p < 0.001$) and the narrow beam ($t_{(13)}$ = 2.188, $p < 0.05$) than the WT mice in the beam walking test (Figure 3A). Similar alterations in motor coordination performance were

14

revealed using the footprint test. MAGL KO mice presented a consistently shorter stride length than WT mice (L forelimb: t (16) = 2.479, p < 0.05; R forelimb: t (16) = 3.289, p < 0.05; L hindlimb: t (16) = 3.087, p < 0.05; R hindlimb: t (16) = 2.695, p < 0.05) (Figure 3B). No significant differences were found in the base width neither in the overlap width as it was found after the JZL184 treatment (data not shown).

Microglial morphology analysis performed in Iba1 immunostained tissues revealed that MAGL deletion produced changes on the microglial cell perimeter in the cerebellar molecular layer of MAGL KO mice compared to the WT group (t (8) = 4.08, p < 0.01) (Figure 4A), whereas no differences were observed in the hippocampal microglial cells of MAGL KO mice (Figure 4B).

Moreover, qRT-PCR analysis showed enhanced *Itgam* mRNA expression in MAGL KO mice compared with control mice (t (14) = 3.902, p < 0.01) (Figure 4C) without significant alteration in the hippocampus (Figure 4D). Although, *Ilb1* and *Tnfa* genes showed a trend to increase in the MAGL KO mice no significant differences were detected between genotypes neither in the cerebellum (Supplementary Figure 3A) nor in the hippocampus (Supplementary Figure 3B). The mRNA expression of the *Cnr1* and *Cnr2* was analyzed in the cerebellum and hippocampus of MAGL KO mice (Supplementary Figure 3, C and D). While no differences in the *Cnr2* expression were found in the MAGL KO mice, a significant enrichment in the expression of *Cnr1* in the cerebellum of MAGL KO mice was observed (Supplementary Figure 3C).

Notably, qRT-PCR analysis for *Cox2* revealed a significant increase in its expression only in the cerebellar region (t (14) = 5.596, p < 0.001) (Figure 4E), but not in the hippocampus (Figure 4F). Conversely, *Abhd6* expression was

found enhanced in the hippocampus (t (14) = 5.5804, p < 0.001) (Figure 4F), but not in the cerebellum of MAGL KO mice (Figure 4E).

Together, these results demonstrate the particular reactiveness of the cerebellum to the 2-AG elevated levels produced by the genetic MAGL inactivation.

3.4. NS398 reduces motor coordination impairment and microglial reactivity in the cerebellum of MAGL KO mice

We used the COX-2 selective inhibitor NS398 to evaluate the role of the specific increase of COX-2 in the cerebellum of the MAGL KO mice. We treated MAGL KO mice and WT littermates sub-chronically during 5 days with NS398 (10mg/kg, i.p; once per day) or its vehicle. Fine motor coordination was evaluated using the beam walking and footprint tests 3 h after the last administration. After behavioral analysis, tissues were collected for cellular and molecular analysis.

We found that NS398 administration significantly reduced the number of foot-slips performed in the narrow beam by the MAGL KO mice (genotype effect: F (1,58) = 5.966, p < 0.05; treatment effect: F (1,58) = 4.371, p < 0.05; interaction: F (1,58) = 4.285, p = 0.043) (Figure 5A). Moreover, NS398 treatment improved the impaired length of the left forelimb stride in the MAGL KO mice, one of the parameters measured in the footprint test (L forelimb: genotype effect: F (1,38) = 15.11, p < 0.001; treatment effect: F (1,38) = 6.106, p < 0.05; interaction: F (1,38) = 0.446, p = 0.508; NS; R forelimb: genotype effect: F (1,38) = 13.74, p < 0.001; L hindlimb: genotype effect: F (1,38) = 11.49, p < 0.01; R hindlimb: genotype effect: F (1,38) = 11.4, p < 0.01) (Figure 5B).

Interestingly, such improvement in coordination was accompanied by a reduction in the cerebellar microglial reactivity after the NS398 administration. The analysis of the microglial cell soma perimeter in the cerebellum revealed a significant normalization in the MAGL KO mice treated sub-chronically with NS398 (genotype effect: $F_{(1,11)}$ = 8.175, $p < 0.05$; treatment effect: $F_{(1,11)}$ = 8.175, $p < 0.05$; interaction: $F_{(1,11)}$ = 11.91, $p < 0.01$) (Figure 5C), while no effects of NS398 treatment were observed in samples from WT mice.

These results reveal that MAGL deletion produces changes in cerebellar microglial reactivity, which are associated with the presence of motor coordination alterations, all prevented with the COX-2 inhibitor NS398. Indeed, a significant positive correlation ($R = -0.569$, $p < 0.05$) was observed between microglial activation (perimeter of the soma) and motor coordination performance (total number of foot-slips) in all groups analyzed (Figure 5 D).

3.5. Endocannabinoid unbalance in MAGL KO mice

In order to understand the effect that NS398 could produce over the endocannabinoid levels in the MAGL KO mice, we analyzed the concentration of the following 2-acyl glycerols and N-acylethanolamines in their cerebellum and hippocampus: 2-AG, 2-LG, 2-OG, AEA, DEA, DHEA, LEA, OEA, PEA, POEA, SEA (Table 1).

These data revealed, as expected, a significant enhancement of endogenous lipids susceptible of being processed by MAGL such as 2-AG, 2-LG, 2-OG, both in the cerebellum (genotype effect of 2-AG : $F_{(1,29)}$ = 829.7, $p < 0.001$; 2-linoleoyl glycerol: $F_{(1,29)}$ = 255.7, $p < 0.001$; 2-oleoyl glycerol: $F_{(1,28)}$ = 91.15 $p < 0.001$) and the hippocampus (genotype effect of 2-AG: $F_{(1,29)}$ = 1232, $p < 0.001$; 2-LG: $F_{(1,29)}$ = 98.32, $p < 0.001$; 2-OG: $F_{(1,29)}$ = 19.47, $p < 0.001$),

17

with the strongest increase in the concentration of 2-AG (ten times more in the hippocampus and seven times more in the cerebellum). Other endocannabinoids and lipid derivatives measured were not affected in the brain areas analyzed. NS398 sub-chronic treatment during 5 days did not modify the endocannabinoid profile in the cerebellum and hippocampus of WT and MAGL KO mice. These results suggest that under our experimental conditions, COX-2 was not involved in the metabolism of endocannabinoids and related compounds.

3.6. MAGL deletion decreases AA, PGD$_2$ and PGE$_2$ levels in the cerebellum and hippocampus

Genetic or pharmacological inhibition of MAGL produces elevated levels of 2-AG and reductions in AA and its derived prostaglandins as determined in whole brain homogenates (Nomura et al., 2011). We hypothesized that hippocampus and cerebellum could be responding differently to the accumulation of 2-AG in MAGL KO mice. Thus, we measured AA, PGD$_2$ and PGE$_2$ levels in the cerebellum and hippocampus of MAGL KO and WT mice treated sub-chronically with vehicle or NS398 (10 mg/kg; 5 days) (Table 2). We observed a significant decrease in the AA levels in cerebellar (genotype effect: $F_{(1,26)}$ = 222.1, $p < 0.001$) and hippocampal (genotype effect: $F_{(1,26)}$ = 446.3, $p < 0.001$) tissues from MAGL KO compared to WT mice. PGD$_2$ and PGE$_2$ levels were reduced as well in to the same degree in both brain areas (genotype effect of PGD$_2$ in the cerebellum: $F_{(1,25)}$ = 86.05, $p < 0.001$ and hippocampus: $F_{(1,25)}$ = 57.41, $p < 0.001$; genotype effect of PGE$_2$ in the cerebellum: $F_{(1,26)}$ = 37.87, $p < 0.001$ and hippocampus: $F_{(1,25)}$ = 30.37, $p < 0.001$). Interestingly, NS398 sub-chronic treatment did not alter AA, PGD$_2$ or PGE$_2$ levels in MAGL

KO mice. Together, these results suggested that PGD_2 and PGE_2 are not involved in the microglial activation detected after genetic or pharmacological MAGL inhibition in the cerebellum. However, we could not discard that other prostaglandins produced by COX-2 such as the PG-Gs, which are unstable *in vivo* and therefore difficult to detect (Kingsley et al., 2005; Kozak et al., 2001) might be implicated in this process.

4. Discussion

This study describes the consequences of the pharmacological inhibition and genetic inactivation of MAGL on motor coordination, microglial reactivity and inflammatory mediators of relevant brain regions. The inflammatory state that we observe in the cerebellum of JZL184-treated and MAGL KO mice has a profound relevance in its functionality, where COX-2 would have a considerable participation. Such molecular alterations were not observed in the hippocampus, pointing to a particular sensitivity of the cerebellum to the local inflammatory processes promoted by the enhancement of 2-AG.

2-AG is the most abundant endocannabinoid in the brain acting as a full agonist of both CB1 and CB2 receptors (CB1R and CB2R) (Nakane et al., 2002) and mainly hydrolyzed by MAGL (Bisogno et al., 1999). Usually, physiological levels of synaptic endocannabinoids are responsible for different forms of short-term synaptic plasticity (Araque et al., 2017). Elevated physiological levels of endocannabinoids are produced upon injury, and this production is thought to have protective roles aiming at decreasing pro-inflammatory mediators, reducing microglial reactivity and prompting brain homeostasis (Xu and Chen, 2015). Therefore, the inhibition of endocannabinoid catabolism has been hypothesized to be useful against inflammation (Alhouayek et al., 2014; Petrosino and Di Marzo, 2010), neurodegeneration (Pihlaja et al., 2015) or oligodendrocyte degeneration (Bernal-Chico et al., 2015). This is in contrast with our observations of enhanced cerebellar inflammation associated to MAGL pharmacological and genetic inhibition. Other enzymes, such as ABHD6 are also involved, although to a minor extent, in 2-AG degradation (Blankman et al., 2007; Marrs et al., 2010). Indeed, it was demonstrated that ABHD6 inhibition was able to reduce microglial reactivity and COX-2 expression in mouse models

of experimental autoimmune encephalomyelitis (Wen et al., 2015) and traumatic brain injury (Tchantchou and Zhang, 2013). Thus, we could not discard that ABHD6 inhibition could reduce the cerebellar microglial reactivity and the motor impairments.

Together, MAGL and ABHD6 turn 2-AG into AA and glycerol. Then, AA is available for prostanoid conversion, through a rate-limiting enzymatic process. Prostanoid production, whether through constitutive COX-1 or inducible COX-2, depends on AA availability (Smith et al., 2011). Therefore, AA pool reduction, as that observed after MAGL inhibition was proposed to prevent inflammatory processes by limiting prostanoid production (Nomura et al., 2011). Interestingly, our data also reveals the reduction in AA, PGE_2 and PGD_2 both in the cerebellum and hippocampus as a result of MAGL inhibition.

COX-2 activity in the brain has been found significant beyond inflammation. In the cerebellum, COX-2 activity was found relevant for long-term synaptic plasticity of Purkinje cells and also for motor learning (Le et al., 2010). In the hippocampus, COX-2 expression seems to be physiologically regulated to contribute to synaptic activity in forebrain dendrites (Chen et al., 2002; Kaufmann et al., 1996). We found that pharmacological and genetic inactivation of MAGL resulted in somewhat different responses in the cerebellum and hippocampus of the same animals according to *Cox2* mRNA expression. Despite both MAGL KO and JZL184 (40 mg/kg)-treated mice showed enhanced cerebellar *Cox2* expression as well as modifications in the microglial morphology and motor coordination impairments, these alterations were exacerbated in the MAGL KO mice. Therefore, we analyzed the impact of the COX-2 inhibition by administering the COX-2 inhibitor NS398 to the MAGL KO mice, expecting similar effects in the JZL184 (40 mg/kg)-treated mice where the

molecular and behavioral alterations were less evident. We found that NS398 sub-chronic administration prevented the motor coordination impairments and the microglial reactivity detected in the MAGL KO mice. Moreover, NS398 sub-chronic administration did not alter the levels of PGE_2 and PGD_2, discarding their involvement in microglial reactivity. Conversely, although the hippocampus showed the expected blunted levels of AA, PGE_2 and PGD_2, it did not show alterations on the microglial reactivity. In fact, MAGL inhibition has been shown to improve hippocampal functioning, as revealed by others through behavioral and synaptic plasticity analysis (Hashimotodani et al., 2007; Kishimoto et al., 2015) pointing to a differential effect of MAGL inhibition among different brain areas.

Previous studies demonstrated that MAGL inactivation produced elevations in 2-AG levels and significant reductions in AA levels and in its downstream-derived eicosanoids in brain homogenates (Leishman et al., 2016; Nomura et al., 2011). The differential response between cerebellum and hippocampus may derive from the alternative metabolism of accumulated 2-AG in both brain areas (Supplementary Figure 4). This endocannabinoid can be processed by COX-2 to produce PG-Gs. This enzymatic reaction first described *in vitro* (Alhouayek and Muccioli, 2014; Kozak et al., 2002) has been recently observed *in vivo* under conditions of enhanced 2-AG accumulation (Hu et al., 2008; Kingsley et al., 2005; Morgan et al., 2018). These PG-Gs derived from 2-AG buildup would act through classical prostanoid receptors (Kozak et al., 2001), and alternative receptors (Hu et al., 2008). In this regard, nucleotide receptor P2Y6 may be activated by PG-Gs, and particularly by PGE_2-G with high affinity agonist/receptor pair (Brüser et al., 2017). Moreover, P2Y6 receptor is expressed in microglial cells where it mediates inflammation, migration and

phagocytosis in normal and pathophysiological conditions (Barragán-Iglesias et al., 2014; Koizumi et al., 2007). Such a mediator could be involved as a link between the putative raise of PG-Gs derived from 2-AG by COX-2 activity, and the microglial reactivity detected in our study specifically in the cerebellum. Further studies are required to clearly identify the mechanisms involved in this link.

Despite that microglial reactivity after MAGL inactivation was clearly revealed by microglial morphology and the increased expression of *Itgam* mRNA, only subtle changes in the mRNA of *Il1b* and *Tnfa* were detectable in the cerebellum of JZL184-treated and MAGL KO mice. This is in agreement with previous observations in whole brain homogenates after pharmacological and genetic inhibition of MAGL (Nomura et al., 2011) showing no alteration of basal mRNA levels of *Il1b*, *Il1a*, *Il6* and *Tnfa*. It is plausible that together with the production of COX-2-dependent pro-inflammatory PG-Gs, 2-AG may also act through CB2R expressed in reactive microglia to prevent full microglial activation. Indeed, 2-AG may act as an agonist of the microglial CB2R and modulate the microglial reactivity as well, as previously described in other inflammatory situations (Maresz et al., 2005; Wen et al., 2015). Therefore, a balance between activation and inactivation state might exist on the microglial cells of MAGL KO mice. This hypothesis may explain why MAGL inactivation is able to mediate changes in the microglial morphology, but not to impact in the translation of pro-inflammatory cytokines. Moreover, while no important differences in the *Cnr2* expression were found in the MAGL KO mice neither in cerebellum nor in hippocampus, a significant enrichment in the expression of *Cnr1* in the cerebellum of MAGL KO mice was observed, suggesting the specific response

23

of the cerebellum to the MAGL inhibition and the subsequent 2-AG content increase.

Several publications show the neuroprotective effects of pharmacological MAGL inhibition by using JZL184 (Chen et al., 2012; Lysenko et al., 2014; Nomura et al., 2011), KML29 (Pasquarelli et al., 2017b, 2017a) or MJN110 (Niphakis et al., 2013). These promising features of MAGL inhibition are somewhat contradictory with the present results and previous work (Cutando et al., 2013) demonstrating the presence of activated microglia and motor coordination deficits under conditions of increased cannabinergic tone. In fact, the administration of KML29 (Chang et al., 2012) or MJN110 (Niphakis et al., 2013) does not show untoward side effects on the motor coordination. However, it still remains to be clarified whether these highly-selective MAGL-inhibitors trigger microglial reactivity in the cerebellum. Although we cannot discard unforeseen adaptations during development in the MAGL KO model, these mice and JZL184 (40 mg/kg)-treated mice showed correlative modifications suggesting that an important part of the effects observed with the JZL184 administration are mediated through MAGL inhibition. The cellular localization of MAGL is an additionally relevant aspect, since MAGL expressed in Purkinje cells was shown to be responsible for the direct effects of inhibitors to cause cerebellar motor coordination alterations (Suárez et al., 2008).

Altogether, the present study reveals the sensitivity of the cerebellum to alterations in ECS signaling, compared to other brain areas such as the hippocampus, and highlights a potential drawback of strategies directed to the inhibition of the MAGL activity as a target for inflammatory disorders.

Figure legends

Figure 1. Acute JZL184 administration produces motor coordination deficits in mice. (A) Number of foot-slips in the wide and narrow beam and **(B)** footprint parameters obtained 6h after acute administration of VEH, JZL184 (8 mg/kg) or JZL184 (40 mg/kg) (n = 5-7 mice per group). Distribution of individual data with mean ± SEM Dara were analyzed by one-way ANOVA test followed by Bonferroni post hoc. *p < 0.05, **p < 0.01 as compared to VEH.

Figure 2. Inhibition of MAGL with JZL184 reveals cerebellar neuroinflammation in mice. Morphological analysis of Iba1 cells and its representative images from the cerebellar molecular layer **(A)** and CA3 region of the hippocampus **(B)** 6h after VEH, JZL184 (8mg/kg) and JZL184 (40 mg/kg) treatment (n = 5-6 mice per group) Scale bar represents 25µm. Analysis of mRNA expression of *Itgam* by qRT-PCR in the cerebellum **(C)** and hippocampus **(D)** of JZL184 (8mg/kg), JZL184 (40mg/kg) and vehicle treated groups (n = 4-6 mice per group). Expression of *Cox2* and *Abhd6* mRNA by qRT-PCR in the cerebellum **(E)** and hippocampus **(F)** of JZL184 (8mg/kg), JZL184 (40 mg/kg) and vehicle treated groups (n = 4-6 mice per group). Distribution of individual data with mean ± SEM. Data were analyzed by one-way ANOVA test followed by Bonferroni post hoc. *p < 0.05 as compared to VEH.

Figure 3. Impaired motor coordination in MAGL KO mice. (A) Total number of foot-slips in the beam walking test and **(B)** Footprint parameters obtained in WT and MAGL KO mice (n = 7-11 mice per group). Distribution of individual data with mean ± SEM. Data were analyzed by Student's *t*-test. *p<0.05 and **p<0.01 WT versus MAGL KO mice.

Figure 4. MAGL KO mice show cerebellar neuroinflammation. Iba1 immunostaining of **(A)** cerebellar and **(B)** hippocampal microglial cells (n = 4-5 mice per group) Scale bar represents 25µm. Analysis of *Itgam* mRNAs expression by qRT-PCR in the **(C)** cerebellum and **(D)** hippocampus of MAGL -/- and WT mice (n = 8 mice per group). Quantitative mRNAs expression of *Cox2* and *Abhd6* in the **(E)** cerebellum and **(F)** hippocampus of WT and MAGL -/- mice. Distribution of individual data with mean ± SEM. Data were analyzed by Student's *t*-test. **p < 0.01 and ***p < 0.001 WT versus MAGL KO mice.

Figure 5. NS398 administration prevents the motor impairment and reverses the microglial reactivity in the MAGL KO mice. Motor coordination analysis using the **(A)** beam walking test (n = 12-16 mice per group) and **(B)** footprint test (n = 9-11 mice per group) in WT or MAGL KO mice after 5 days of VEH or NS398 treatment. **(C)** Morphological analysis of Iba1 immunostained cells in the cerebellar molecular layer after NS398 treatment in MAGL KO mice (n = 3-4 mice per group) Scale bar represents 25µm. **(D)** Correlation between motor coordination in the narrow beam of the beam walking test (number of foot-slips) and microglial activation (perimeter of the soma) in the molecular layer of the cerebellum. Distribution of individual data with mean ± SEM. Data were analyzed by two-way ANOVA test followed by Bonferroni post hoc. *p < 0.05 and **p < 0.01 as genotype comparison and [#]p < 0.05 as treatment comparison.

Acknowledgements

Appendix A. Supplementary data

References

Alhouayek, M., Masquelier, J., Muccioli, G.G., 2014. Controlling 2-arachidonoylglycerol metabolism as an anti-inflammatory strategy. Drug Discov. Today 19, 295–304.

Alhouayek, M., Muccioli, G.G., 2014. COX-2-derived endocannabinoid metabolites as novel inflammatory mediators. Trends Pharmacol. Sci. 35, 284–292.

Araque, A., Castillo, P.E., Manzoni, O.J., Tonini, R., 2017. Synaptic functions of endocannabinoid signaling in health and disease. Neuropharmacology 124, 13–24.

Ativie, F., Albayram, O., Bach, K., Pradier, B., Zimmer, A., Bilkei-Gorzo, A., 2015. Enhanced microglial activity in FAAH−/− animals. Life Sci. 138, 52–56.

Barragán-Iglesias, P., Pineda-Farias, J.B., Cervantes-Durán, C., Bravo-Hernández, M., Rocha-González, H.I., Murbartián, J., Granados-Soto, V., 2014. Role of spinal P2Y6 and P2Y11 receptors in neuropathic pain in rats: possible involvement of glial cells. Mol. Pain 10, 29.

Bernal-Chico, A., Canedo, M., Manterola, A., Victoria Sánchez-Gómez, M., Pérez-Samartín, A., Rodríguez-Puertas, R., Matute, C., Mato, S., 2015. Blockade of monoacylglycerol lipase inhibits oligodendrocyte excitotoxicity and prevents demyelination in vivo. Glia 63, 163–76.

Bisogno, T., Berrendero, F., Ambrosino, G., Cebeira, M., Ramos, J.A., Fernandez-Ruiz, J.J., Di Marzo, V., 1999. Brain regional distribution of endocannabinoids: implications for their biosynthesis and biological function. Biochem. Biophys. Res. Commun. 256, 377–80.

Blankman, J.L., Simon, G.M., Cravatt, B.F., 2007. A comprehensive profile of brain enzymes that hydrolyze the endocannabinoid 2-arachidonoylglycerol. Chem. Biol. 14, 1347–56.

Brüser, A., Zimmermann, A., Crews, B.C., Sliwoski, G., Meiler, J., König, G.M., Kostenis, E., Lede, V., Marnett, L.J., Schöneberg, T., 2017. Prostaglandin E2 glyceryl ester is an endogenous agonist of the nucleotide receptor P2Y6. Sci. Rep. 7, 2380.

Busquets-Garcia, A., Puighermanal, E., Pastor, A., de la Torre, R., Maldonado, R., Ozaita, A., 2011. Differential role of anandamide and 2-arachidonoylglycerol in memory and anxiety-like responses. Biol. Psychiatry 70, 479–86.

Chang, J.W., Niphakis, M.J., Lum, K.M., Cognetta, A.B., Wang, C., Matthews, M.L., Niessen, S., Buczynski, M.W., Parsons, L.H., Cravatt, B.F., Cravatt, B.F., 2012. Highly selective inhibitors of monoacylglycerol lipase bearing a reactive group that is bioisosteric with endocannabinoid substrates. Chem. Biol. 19, 579–88.

Chen, C., Magee, J.C., Bazan, N.G., 2002. Cyclooxygenase-2 Regulates Prostaglandin E $_2$ Signaling in Hippocampal Long-Term Synaptic Plasticity.

J. Neurophysiol. 87, 2851–2857.

Chen, R., Zhang, J., Wu, Y., Wang, D., Feng, G., Tang, Y.-P., Teng, Z., Chen, C., 2012. Monoacylglycerol Lipase Is a Therapeutic Target for Alzheimer's Disease. Cell Rep. 2, 1329–1339.

Cravatt, B.F., Giang, D.K., Mayfield, S.P., Boger, D.L., Lerner, R.A., Gilula, N.B., 1996. Molecular characterization of an enzyme that degrades neuromodulatory fatty-acid amides. Nature 384, 83–7.

Cutando, L., Busquets-Garcia, A., Puighermanal, E., Gomis-González, M., Delgado-García, J.M., Gruart, A., Maldonado, R., Ozaita, A., 2013. Microglial activation underlies cerebellar deficits produced by repeated cannabis exposure. J. Clin. Invest. 123, 2816–2831.

Dinh, T.P., Freund, T.F., Piomelli, D., 2002. A role for monoglyceride lipase in 2-arachidonoylglycerol inactivation. Chem. Phys. Lipids 121, 149–58.

Gao, Y., Vasilyev, D. V, Goncalves, M.B., Howell, F. V, Hobbs, C., Reisenberg, M., Shen, R., Zhang, M.-Y., Strassle, B.W., Lu, P., Mark, L., Piesla, M.J., Deng, K., Kouranova, E. V, Ring, R.H., Whiteside, G.T., Bates, B., Walsh, F.S., Williams, G., Pangalos, M.N., Samad, T.A., Doherty, P., 2010. Loss of retrograde endocannabinoid signaling and reduced adult neurogenesis in diacylglycerol lipase knock-out mice. J. Neurosci. 30, 2017–24.

Hashimotodani, Y., Ohno-Shosaku, T., Kano, M., 2007. Presynaptic monoacylglycerol lipase activity determines basal endocannabinoid tone and terminates retrograde endocannabinoid signaling in the hippocampus. J. Neurosci. 27, 1211–9.

Hu, S.S.-J., Bradshaw, H.B., Chen, J.S.-C., Tan, B., Walker, J.M., 2008. Prostaglandin E2 glycerol ester, an endogenous COX-2 metabolite of 2-arachidonoylglycerol, induces hyperalgesia and modulates NFkappaB activity. Br. J. Pharmacol. 153, 1538–49.

Kano, M., Ohno-Shosaku, T., Hashimotodani, Y., Uchigashima, M., Watanabe, M., 2009. Endocannabinoid-Mediated Control of Synaptic Transmission. Physiol. Rev. 89, 309–380.

Katz, P.S., Sulzer, J.K., Impastato, R.A., Teng, S.X., Rogers, E.K., Molina, P.E., 2015. Endocannabinoid degradation inhibition improves neurobehavioral function, blood-brain barrier integrity, and neuroinflammation following mild traumatic brain injury. J. Neurotrauma 32, 297–306.

Kaufmann, W.E., Worley, P.F., Pegg, J., Bremer, M., Isakson, P., 1996. COX-2, a synaptically induced enzyme, is expressed by excitatory neurons at postsynaptic sites in rat cerebral cortex. Proc. Natl. Acad. Sci. U. S. A. 93, 2317–21.

Kilkenny, C., Browne, W., Cuthill, I.C., Emerson, M., Altman, D.G., NC3Rs Reporting Guidelines Working Group, 2010. Animal research: Reporting in vivo experiments: The ARRIVE guidelines. Br. J. Pharmacol. 160, 1577–1579.

Kingsley, P.J., Rouzer, C.A., Saleh, S., Marnett, L.J., 2005. Simultaneous

analysis of prostaglandin glyceryl esters and prostaglandins by electrospray tandem mass spectrometry. Anal. Biochem. 343, 203–211.

Kishimoto, Y., Cagniard, B., Yamazaki, M., Nakayama, J., Sakimura, K., Kirino, Y., Kano, M., 2015. Task-specific enhancement of hippocampus-dependent learning in mice deficient in monoacylglycerol lipase, the major hydrolyzing enzyme of the endocannabinoid 2-arachidonoylglycerol. Front. Behav. Neurosci. 9, 134.

Koizumi, S., Shigemoto-Mogami, Y., Nasu-Tada, K., Shinozaki, Y., Ohsawa, K., Tsuda, M., Joshi, B. V, Jacobson, K.A., Kohsaka, S., Inoue, K., 2007. UDP acting at P2Y6 receptors is a mediator of microglial phagocytosis. Nature 446, 1091–5.

Kozak, K.R., Crews, B.C., Morrow, J.D., Wang, L.-H., Ma, Y.H., Weinander, R., Jakobsson, P.-J., Marnett, L.J., 2002. Metabolism of the Endocannabinoids, 2-Arachidonylglycerol and Anandamide, into Prostaglandin, Thromboxane, and Prostacyclin Glycerol Esters and Ethanolamides. J. Biol. Chem. 277, 44877–44885.

Kozak, K.R., Prusakiewicz, J.J., Rowlinson, S.W., Schneider, C., Marnett, L.J., 2001. Amino acid determinants in cyclooxygenase-2 oxygenation of the endocannabinoid 2-arachidonylglycerol. J. Biol. Chem. 276, 30072–7.

Le, T.D., Shirai, Y., Okamoto, T., Tatsukawa, T., Nagao, S., Shimizu, T., Ito, M., 2010. Lipid signaling in cytosolic phospholipase A2alpha-cyclooxygenase-2 cascade mediates cerebellar long-term depression and motor learning. Proc. Natl. Acad. Sci. U. S. A. 107, 3198–203.

Leishman, E., Cornett, B., Spork, K., Straiker, A., MacKie, K., Bradshaw, H.B., 2016. Broad impact of deleting endogenous cannabinoid hydrolyzing enzymes and the CB1 cannabinoid receptor on the endogenous cannabinoid-related lipidome in eight regions of the mouse brain. Pharmacol. Res. 110, 159–172.

Long, J.Z., Li, W., Booker, L., Burston, J.J., Kinsey, S.G., Schlosburg, J.E., Pavón, F.J., Serrano, A.M., Selley, D.E., Parsons, L.H., Lichtman, A.H., Cravatt, B.F., 2009a. Selective blockade of 2-arachidonoylglycerol hydrolysis produces cannabinoid behavioral effects. Nat. Chem. Biol. 5, 37–44.

Long, J.Z., Nomura, D.K., Cravatt, B.F., 2009b. Characterization of monoacylglycerol lipase inhibition reveals differences in central and peripheral endocannabinoid metabolism. Chem. Biol. 16, 744–53.

Lysenko, L. V, Kim, J., Henry, C., Tyrtyshnaia, A., Kohnz, R.A., Madamba, F., Simon, G.M., Kleschevnikova, N.E., Nomura, D.K., Ezekowitz, R.A.B., Kleschevnikov, A.M., 2014. Monoacylglycerol lipase inhibitor JZL184 improves behavior and neural properties in Ts65Dn mice, a model of down syndrome. PLoS One 9, e114521.

Maresz, K., Carrier, E.J., Ponomarev, E.D., Hillard, C.J., Dittel, B.N., 2005. Modulation of the cannabinoid CB2 receptor in microglial cells in response to inflammatory stimuli. J. Neurochem. 95, 437–45.

Marrs, W.R., Blankman, J.L., Horne, E.A., Thomazeau, A., Lin, Y.H., Coy, J., Bodor, A.L., Muccioli, G.G., Hu, S.S.-J., Woodruff, G., Fung, S., Lafourcade, M., Alexander, J.P., Long, J.Z., Li, W., Xu, C., Möller, T., Mackie, K., Manzoni, O.J., Cravatt, B.F., Stella, N., 2010. The serine hydrolase ABHD6 controls the accumulation and efficacy of 2-AG at cannabinoid receptors. Nat. Neurosci. 13, 951–7.

Morgan, A.J., Kingsley, P.J., Mitchener, M.M., Altemus, M., Patrick, T.A., Gaulden, A.D., Marnett, L.J., Patel, S., 2018. Detection of Cyclooxygenase-2-Derived Oxygenation Products of the Endogenous Cannabinoid 2-Arachidonoylglycerol in Mouse Brain. ACS Chem. Neurosci. 9, 1552–1559.

Nakane, S., Oka, S., Arai, S., Waku, K., Ishima, Y., Tokumura, A., Sugiura, T., 2002. 2-Arachidonoyl-sn-glycero-3-phosphate, an arachidonic acid-containing lysophosphatidic acid: occurrence and rapid enzymatic conversion to 2-arachidonoyl-sn-glycerol, a cannabinoid receptor ligand, in rat brain. Arch. Biochem. Biophys. 402, 51–8.

Navarro-Romero, A., Vázquez-Oliver, A., Gomis-González, M., Garzón-Montesinos, C., Falcón-Moya, R., Pastor, A., Martín-García, E., Pizarro, N., Busquets-Garcia, A., Revest, J.-M., Piazza, P.-V., Bosch, F., Dierssen, M., de la Torre, R., Rodríguez-Moreno, A., Maldonado, R., Ozaita, A., 2019. Cannabinoid type-1 receptor blockade restores neurological phenotypes in two models for Down syndrome. Neurobiol. Dis. 125, 92–106.

Niphakis, M.J., Cognetta, A.B., Chang, J.W., Buczynski, M.W., Parsons, L.H., Byrne, F., Burston, J.J., Chapman, V., Cravatt, B.F., 2013. Evaluation of NHS carbamates as a potent and selective class of endocannabinoid hydrolase inhibitors. ACS Chem. Neurosci. 4, 1322–32.

Nomura, D.K., Morrison, B.E., Blankman, J.L., Long, J.Z., Kinsey, S.G., Marcondes, M.C.G., Ward, A.M., Hahn, Y.K., Lichtman, A.H., Conti, B., Cravatt, B.F., 2011. Endocannabinoid Hydrolysis Generates Brain Prostaglandins That Promote Neuroinflammation. Science (80-.). 334, 809–813.

Ohno-Shosaku, T., Kano, M., 2014. Endocannabinoid-mediated retrograde modulation of synaptic transmission. Curr. Opin. Neurobiol. 29, 1–8.

Pasquarelli, N., Engelskirchen, M., Hanselmann, J., Endres, S., Porazik, C., Bayer, H., Buck, E., Karsak, M., Weydt, P., Ferger, B., Witting, A., 2017a. Evaluation of monoacylglycerol lipase as a therapeutic target in a transgenic mouse model of ALS. Neuropharmacology 124, 157–169.

Pasquarelli, N., Porazik, C., Bayer, H., Buck, E., Schildknecht, S., Weydt, P., Witting, A., Ferger, B., 2017b. Contrasting effects of selective MAGL and FAAH inhibition on dopamine depletion and GDNF expression in a chronic MPTP mouse model of Parkinson's disease. Neurochem. Int. 110, 14–24.

Petrosino, S., Di Marzo, V., 2010. FAAH and MAGL inhibitors: therapeutic opportunities from regulating endocannabinoid levels. Curr. Opin. Investig. Drugs 11, 51–62.

Pihlaja, R., Takkinen, J., Eskola, O., Vasara, J., López-Picón, F.R., Haaparanta-

Solin, M., Rinne, J.O., 2015. Monoacylglycerol lipase inhibitor JZL184 reduces neuroinflammatory response in APdE9 mice and in adult mouse glial cells. J. Neuroinflammation 12, 1–6.

Rivera, P., Arrabal, S., Cifuentes, M., Grondona, J.M., Pérez-Martín, M., Rubio, L., Vargas, A., Serrano, A., Pavón, F.J., Suárez, J., Rodríguez de Fonseca, F., 2014. Localization of the cannabinoid CB1 receptor and the 2-AG synthesizing (DAGLα) and degrading (MAGL, FAAH) enzymes in cells expressing the Ca(2+)-binding proteins calbindin, calretinin, and parvalbumin in the adult rat hippocampus. Front. Neuroanat. 8, 56.

Saravia, R., Flores, Á., Plaza-Zabala, A., Busquets-Garcia, A., Pastor, A., de la Torre, R., Di Marzo, V., Marsicano, G., Ozaita, A., Maldonado, R., Berrendero, F., 2017. CB1 Cannabinoid Receptors Mediate Cognitive Deficits and Structural Plasticity Changes During Nicotine Withdrawal. Biol. Psychiatry 81, 625–634.

Savinainen, J.R., Saario, S.M., Laitinen, J.T., 2012. The serine hydrolases MAGL, ABHD6 and ABHD12 as guardians of 2-arachidonoylglycerol signalling through cannabinoid receptors. Acta Physiol. 204, 267–276.

Smith, W.L., Urade, Y., Jakobsson, P.-J., 2011. Enzymes of the cyclooxygenase pathways of prostanoid biosynthesis. Chem. Rev. 111, 5821–65.

Suárez, J., Bermúdez-Silva, F.J., Mackie, K., Ledent, C., Zimmer, A., Cravatt, B.F., de Fonseca, F.R., 2008. Immunohistochemical description of the endogenous cannabinoid system in the rat cerebellum and functionally related nuclei. J. Comp. Neurol. 509, 400–21.

Tanimura, A., Uchigashima, M., Yamazaki, M., Uesaka, N., Mikuni, T., Abe, M., Hashimoto, K., Watanabe, M., Sakimura, K., Kano, M., 2012. Synapse type-independent degradation of the endocannabinoid 2-arachidonoylglycerol after retrograde synaptic suppression. Proc. Natl. Acad. Sci. 109, 12195–12200.

Tanimura, A., Yamazaki, M., Hashimotodani, Y., Uchigashima, M., Kawata, S., Abe, M., Kita, Y., Hashimoto, K., Shimizu, T., Watanabe, M., Sakimura, K., Kano, M., 2010. The endocannabinoid 2-arachidonoylglycerol produced by diacylglycerol lipase alpha mediates retrograde suppression of synaptic transmission. Neuron 65, 320–7.

Tchantchou, F., Zhang, Y., 2013. Selective inhibition of alpha/beta-hydrolase domain 6 attenuates neurodegeneration, alleviates blood brain barrier breakdown, and improves functional recovery in a mouse model of traumatic brain injury. J. Neurotrauma 30, 565–79.

Uchigashima, M., Yamazaki, M., Yamasaki, M., Tanimura, A., Sakimura, K., Kano, M., Watanabe, M., 2011. Molecular and Morphological Configuration for 2-Arachidonoylglycerol-Mediated Retrograde Signaling at Mossy Cell-Granule Cell Synapses in the Dentate Gyrus. J. Neurosci. 31, 7700–7714.

Urquhart, P., Nicolaou, A., Woodward, D.F., 2015. Endocannabinoids and their oxygenation by cyclo-oxygenases, lipoxygenases and other oxygenases.

Biochim. Biophys. Acta 1851, 366–376.

Vane, J.R., Botting, R.M., 1998. Anti-inflammatory drugs and their mechanism of action. Inflamm. Res. 47 Suppl 2, S78-87.

Wen, J., Ribeiro, R., Tanaka, M., Zhang, Y., 2015. Activation of CB2 receptor is required for the therapeutic effect of ABHD6 inhibition in experimental autoimmune encephalomyelitis. Neuropharmacology 99, 196–209.

Xu, J.-Y., Chen, C., 2015. Endocannabinoids in synaptic plasticity and neuroprotection. Neuroscientist 21, 152–68.

Table 1. Effect of NS398 in the levels of endocannabinoids and related compounds in the cerebellum and hippocampus of WT and MAGL KO mice.

		CEREBELLUM				HIPPOCAMPUS			
		Vehicle		NS398		Vehicle		NS398	
		WT	MAGL KO	WT	MAGL KO	WT	MAGL KO	WT	MAGL KO
2-acyl glycerols	2-AG (nmol/g tissue)	6.69 ± 0.39	46.75 ± 2.26***	6.6 ± 0.35	49.23 ± 1.60***	11.58 ± 0.82	120.93 ± 4.86***	14.3 ± 0.78	122.13 ± 3.49***
	2-LG (nmol/g tissue)	3.08 ± 0.27	13.13 ± 0.58***	3.29 ± 0.18	14.49 ± 1.05***	2.97 ± 0.3	8.04 ± 0.43***	3.56 ± 0.29	8.97 ± 0.80***
	2-OG (nmol/g tissue)	1.92 ± 0.13	3.75 ± 0.13***	1.93 ± 0.13	4.33 ± 0.34***	3.18 ± 0.29	5.01 ± 0.48***	3.33 ± 0.27	4.81 ± 0.39*
N-acylethanolamines	AEA (pmol/g tissue)	3.10 ± 0.29	2.62 ± 0.25	2.91 ± 0.36	3.02 ± 0.31	5.85 ± 0.41	7.85 ± 1.44	6.74 ± 0.38	8.35 ± 1.69
	DHEA (pmol/g tissue)	11.56 ± 0.66	9.22 ± 0.38	2.12 ± 0.8	11.48 ± 0.97	7.36 ± 0.42	8.3 ± 1.14	8.36 ± 0.36	9.23 ± 1.48
	DEA (pmol/g tissue)	0.84 ± 0.06	0.83 ± 0.06	0.78 ± 0.02	0.76 ± 0.06	0.9 ± 0.08	0.73 ± 0.06	1.02 ± 0.04	1.00 ± 0.17
	LEA (pmol/g tissue)	6.14 ± 0.61	6.90 ± 0.39	5.92 ± 0.38	8.20 ± 0.60	9.61 ± 1.06	11.2 ± 0.49	10.24 ± 0.67	16.42 ± 3.36
	OEA (pmol/g tissue)	139.33 ± 9.26	125.25 ± 4.48	136.71 ± 4.59	134.56 ± 6.69	91.59 ± 9.28	85.17 ± 6.36	87.98 ± 3.87	91.99 ± 9.17
	PEA (pmol/g tissue)	288.44 ± 13.25	267.5 ± 7.09	280.14 ± 8.03	287.67 ± 17.10	231.89 ± 12.38	226.37 ± 15.09	213.17 ± 5.44	238.22 ± 16.99
	POEA (pmol/g tissue)	14.80 ± 1.46	11.39 ± 0.73	13.07 ± 1.16	13.41 ± 0.90	13.34 ± 1.06	14.87 ± 2.12	16.81 ± 1.61	17.91 ± 3.46
	SEA (pmol/g tissue)	121.33 ± 4.41	117 ± 2.56	119.14 ± 3.86	118.67 ± 6.90	80.99 ± 1.61	77.41 ± 3.15	78.38 ± 2.71	81.67 ± 4.19

2-arachidonoyl glycerol (2-AG), 2-linoleoyl glycerol (2-LG), 2-oleoyl glycerol (2-OG), N-arachidonoylethanolamine or anandamide (AEA), N-docosatetraenoylethanolamine (DEA), N-docosahexaenoylethanolamine (DHEA), N-linoleoylethanolamine (LEA), N-oleoylethanolamine (OEA), N-palmitoylethanolamine (PEA), N-palmitoleoylethanolamine (POEA), N-stearoylethanolamine (SEA). Values are expressed as mean ± SEM. Data were analyzed by two-way ANOVA test followed by Bonferroni post hoc. *p < 0.05 and ***p < 0.001 WT versus MAGL KO mice.

Table 2. Effect of NS398 treatment in the arachidonic acid and prostaglandin levels in cerebellar and hippocampal tissue from WT and MAGL KO mice.

	CEREBELLUM				HIPPOCAMPUS			
	Vehicle		NS398		Vehicle		NS398	
	WT	MAGL KO	WT	MAGL KO	WT	MAGL KO	WT	MAGL KO
AA (nmol/g)	25.25 ± 1.54	9.96 ± 3.74***	25.33 ± 0.41	9.36 ± 2.23***	55.75 ± 0.98	23.68 ± 1.73***	57.34 ± 1.53	23.23 ± 2.06***
PGD_2 (pmol/g)	10.62 ± 1.13	3.06 ± 1.97***	11.54 ± 0.82	2.81 ± 0.86***	11.14 ± 1.29	2.46 ± 0.48***	12.31 ± 1.52	2.86 ± 0.65***
PGE_2 (pmol/g)	1.88 ± 0.26	0.55 ± 0.41***	1.83 ± 0.19	0.66 ± 0.14**	2.09 ± 0.26	0.85 ± 0.18**	2.05 ± 0.17	1.19 ± 0.33**

Arachidonic acid (AA), prostaglandin-E2 (PGE_2) and prostaglandin-D2 (PGD_2). Values are expressed as mean ± SEM. Data were analyzed by two-way ANOVA test followed by Bonferroni post hoc. **$p < 0.01$ and ***$p < 0.001$ WT versus MAGL KO mice.
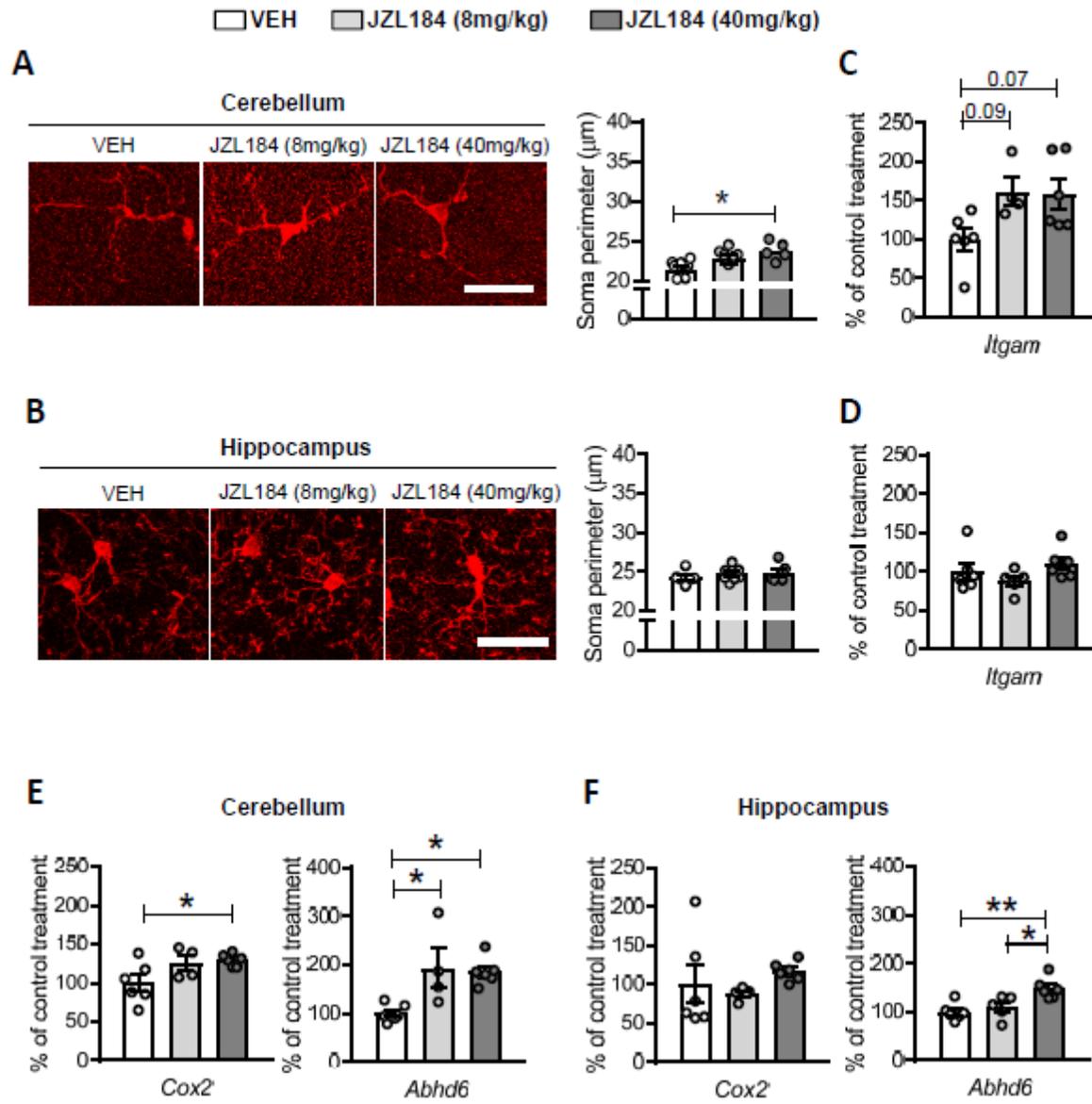
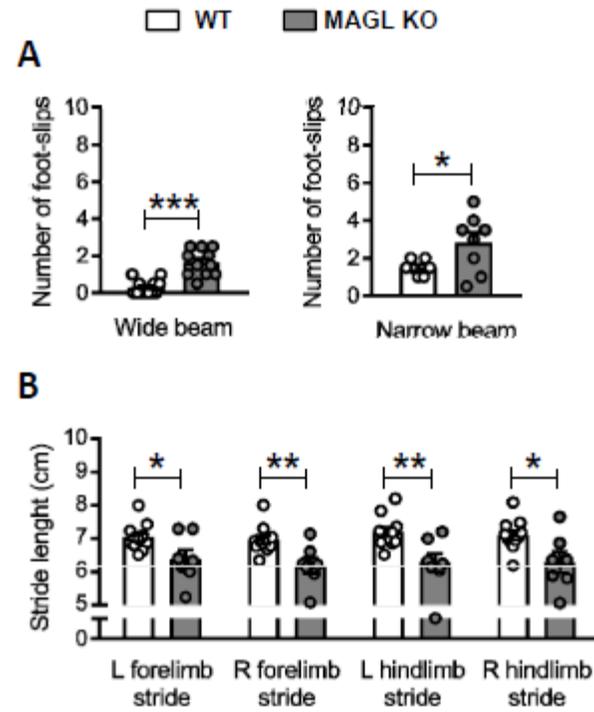**Figure 1.**
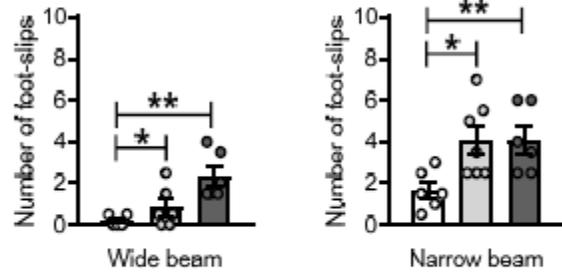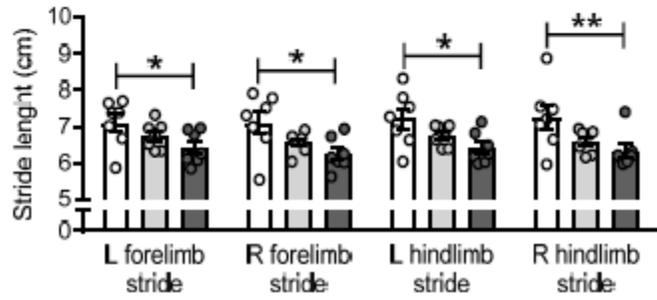
Figure 2.

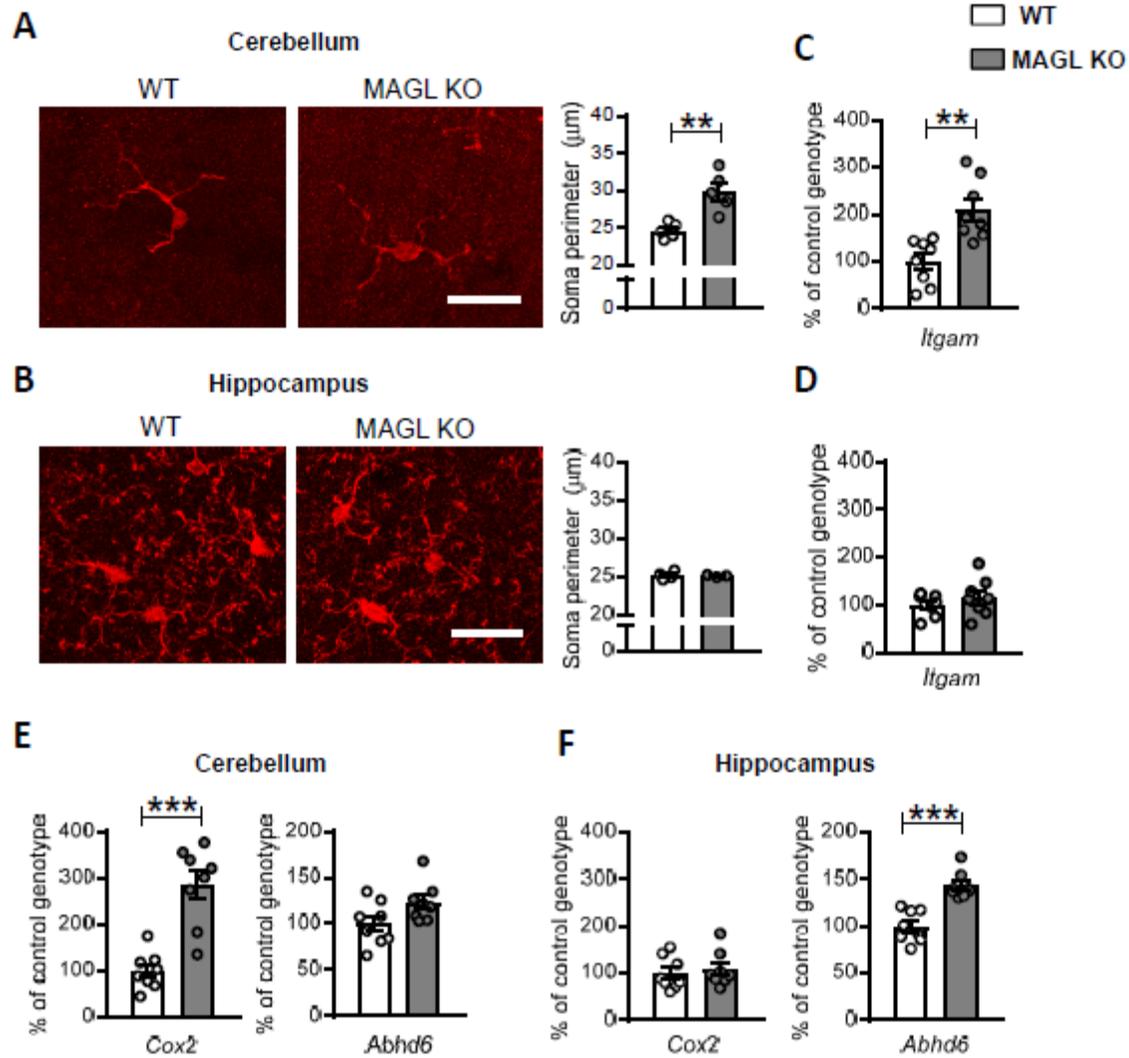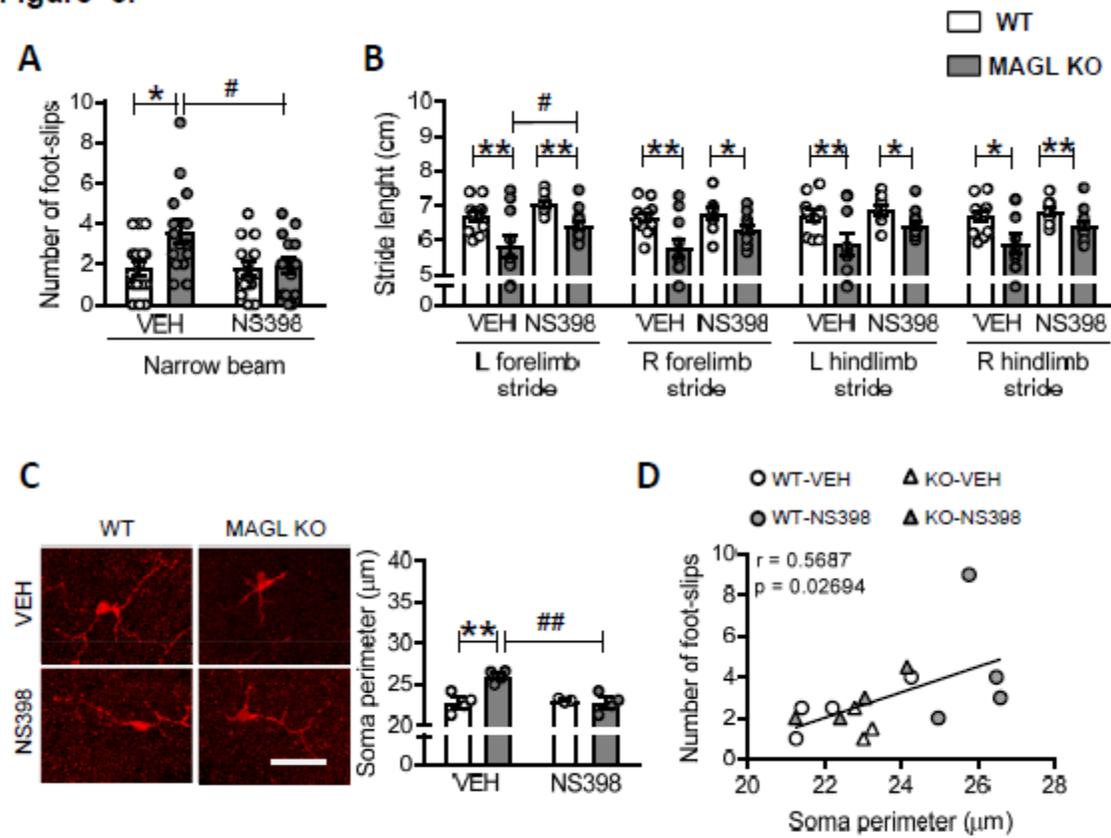**Figure 3.**

Figure 4.

Figure 5.

Highlights

6. Monoacylglycerol lipase (MAGL) inactivation increases microglial perimeter in the cerebellum.

7. Cerebellar microglia activation concurs with COX-2 over-expression and motor deficits.

8. COX-2 inhibition prevents the cerebellar neuroinflammation caused by MAGL deletion.

9. MAGL depletion decreased AA and PGs levels in the cerebellum and hippocampus.

10. Regional differences in MAGL inhibition outcome caution endocannabinoid targeting.